

Optimization of thickness and dye loading time for p25 based dye-sensitized solar cell

Md. Shamimul Haque Choudhury
Department of Electrical and Electronic Engineering
International Islamic University Chittagong (IIUC), Bangladesh

Article info

Keywords

Dye loading time
Dye-Sensitized solar cell
FTO substrate
Photoelectrod
Ruthenium dye

Abstract

In this study, TiO₂-based DSSCs are prepared using the Blade coating technique to find the suitable photoelectrode thickness and optimum dye loading time. The dye loading time is varied from 14 to 26 hours for the photoelectrode thickness of 5 to 30 μm . Photovoltaic performance is measured for the cells under various thicknesses and different dye loading times using a solar simulator. The surface morphology has been observed using a scanning electron microscopy (SEM) image for the photoelectrodes having various thicknesses. The result shows that a smaller thickness of photoelectrode (5 μm) requires relatively less dye loading time of about 14 hours for optimum photoelectric performance. For higher thicknesses (greater than 12 μm), the optimum dye loading time is relatively higher. At 12 μm the maximum solar conversion efficiency has been obtained where the dye loading time was about 18 hours. SEM image confirms a smooth and clean surface morphology for the 12 μm photoelectrode cell compared to other photoelectrode cells.

Corresponding author

Md. Shamimul Haque Choudhury

Department of Electrical and Electronic Engineering, International Islamic University Chittagong, Chattogram, Bangladesh - 4318. Email: shamimul129@gmail.com

1. Introduction

Since the introduction of organic-inorganic Dye-sensitized solar cells (DSSCs) by O'Regan and Grätzel, 1991, DSSCs took substantial attention from researchers. The reason behind the interest in such kind of DSSC is due to its remarkable photovoltaic performance, lower production cost, and less environmental impact (Li & Zhang, 2009). A typical DSSC is composed of a wide bandgap semiconductor film, usually prepared by mesoporous TiO₂ or ZnO nanoparticles having a thickness of 10 to 16 μm for glass substrate-based DSSC (Choudhury, Kishi, & Soga, 2015a,b) and about 6 to 9 μm for flexible DSSC (Fan, Li, Zhou, Miao, Zhang, Hu, & Shao, 2014). These semiconductor films are soaked into a colorful dye solution aimed to yield high light absorption in the range of 400 to 800 nm (Tammy, Qifeng, &

Guozhong, 2007). Other essential components include a liquid electrolyte containing the iodide/triiodide (I^-/I_3^-) redox couple which supplies electrons to the photoelectrode as well as receives electrons from the counter electrode. Electrons are excited by the incident photon and promoted to the conduction band of the metal oxide semiconductor which diffuses through the film and moves toward the counter electrode through the external circuit and reduces the triiodide of the electrolyte. The dye receives electrons from the iodide, thereby closing the cycle of photovoltaic conversion.

Numerous investigations were done by various researchers to improve the cell performance and the overall power conversion efficiency of TiO_2 -based cells reached 14% (Babar, et al., 2020; Lee, Li, & Ho, 2017). Still, the overall power conversion efficiency and stability are lower than the conventional Silicon-based inorganic solar cells. Therefore, more investigations are required for such kinds of solar cells. Photoelectrode preparation is one of the most significant tasks to get highly efficient and stable TiO_2 -based DSSC. Several photoelectrode preparation methods (Lindström, Holmberg, Magnusson, Lindquist, Malmqvist, & Hagfeldt, 2001; Choudhury, Kishi, & Soga, 2015b) along with doping (Abuelwafa, Choudhury, Dongol, El-Nahass, & Soga, 2018; Choudhury, Kishi, Kato, & Soga, 2017) and various post-deposition treatments (Choudhury, Kishi, & Soga, 2016a,b,c) has been performed to get suitable photoelectrode surface as well as improved photoconversion efficiency. Besides, the design and production of photoelectrode (Rahman, Islam, Alam, Uddin, Soga, & Choudhury, 2022), choice of proper liquid dye, a mechanism for maximum dye loading with higher light scattering, better charge transportability, and reduced recombination are the leading challenges in this field of research. The most common choice for photoelectrode materials are TiO_2 , ZnO , Nb_2O_5 , SnO_2 (Etxebarria, Ajuria, & Pacios, 2015; Qiu, Ono, & Qi, 2018; Iwata, Shibakawa, Imawaka, & Yoshino, 2018) porous nanoparticles. Researchers have focused on preparing a homogenous compact layer photoelectrode with suitable doping and with various postdeposition treatments to improve the overall power conversion efficiency and stability. The most common postdeposition treatments include annealing (Choudhury, Kishi, & Soga, 2015b, application of mechanical compression (Meen, Tsai, Tu, Wu, Hsu, & Chang, 2014; Choudhury, Kishi, & Soga, 2016a), and hot compression (Choudhury, Kishi, & Soga, 2016b) which shows improvement in the performance of the cells as reported by the researchers.

The primary focus of the researchers was on the photovoltaic device structure and material properties to enhance the power conversion efficiency

rather than considering the stability. After achieving a moderate level of power conversion efficiency researchers are now focusing on the stability of such solar cells. The main principle of increasing the efficiency of DSSC is based on enhancing the incident photon and effective interaction with the nanoporous metal oxide electrode. Here, colorful monolayer dye molecules are used for enhancing the light scattering phenomenon. Thus, an effective method of photoelectrode fabrication is preferable which will increase the light scattering in the photoanode structure (De Marco, et al., 2010), also ensure effective interaction between the incident photon and dye molecules. The Preparation of metal oxide with a suitable structure is the prime task for such kinds of solar cells. Several methods reported by the researchers to prepare described properties in the use of one-dimensional metal oxides such as nanorods (De Marco, et al., 2010), nanowires (Tan, & Wu, 2006), nanotubes (Luo, Gao, Sun, & Liu, 2012; Sun, Qadir, & Jeong, 2014) nanofibers (Lin, Lin, Lee, & Chen-Yang, 2013), and nanospindles (Wu, Zhu, Li, Dong, Li, Jiang, & Xu, 2012). Later on, hybrid layers of 1D, 2D, and 3D nanostructures were synthesized by the researchers which offer enhanced surface area as well as higher dye loading. For fabricating an efficient solar cell two vital factors such as a high diffusion coefficient and low recombination have a significant role. Increased thickness ensures greater dye loading and higher surface area for light absorption. Therefore, attempts were taken to increase the thickness to improve the photovoltaic performance. On the contrary, higher thickness causes a reduced diffusion coefficient and a higher rate of recombination which in turn causes the reduction of power conversion efficiency. For that reason, a suitable choice of dye as well as proper procedure of dye loading, size of the metal oxide, and optimum photoelectrode layer thickness are the curtail factors for the performance of DSSC. Dye loading is a very essential factor for the efficient light harvesting of a DSSC. A monolayer uniform dye loading is preferable to get better cell performance. Indeed, the formation of multilayer dye alone with a poor dye distribution severely hinders the electron transfer process. Multilayer dye causes agglomeration which in turn increases the charge transfer resistance, reduces the effective electron injection process, and favors undesirable recombination of electrons (Rajab, F. M., 2016). To achieve higher cell efficiency, we need to ensure higher surface area by enhancing the metal oxide thickness as well as to maintain higher diffusion length and lower recombination. In summary, metal oxide film thickness greater than an optimum value leads to reduce electron diffusion lengths and increases electron recombination. Effect of N3 dye concentration and N3 dye loading time for both TiO₂ and ZnO-based DSSC has been investigated where the

efficiency varied from 0.29 to 2.89% (Tammy, Qifeng, & Guozhong, 2007). They also reported the effect of dye concentration as an effect of photoelectrode immersion time at maximum power conversion efficiency. Effect of dye loading time (3, 6 and 9 hour) for two specific dyes named N719 and N749 for TiO_2 -based DSSC was reported by a group of researchers where the optimized thickness was reported about $9\ \mu\text{m}$ (Rajib, F. M., 2016). The highest power conversion efficiency was found at 9-hour dye loading time for both of the dyes. However, they could not report the optimized time for dye loading as they did not investigate the performance of the cells where the electrodes loaded in a dye for more than 9 hours. In another report, effect of dye loading time (various types of turmeric dye) for TiO_2 -based DSSC has been reported where the obtained power conversion efficiency varied from 0.15 to 0.34% (Hossain, et al., 2017). N179 dye has been used for various dye loading time (1 to 24 h) for ZnO-based DSSC where the number of depositing layers were varied (Magiswaran, et al., 2022). As per their report the maximum power conversion efficiency was found about 2.77% for 3 hours of dye loading time where the number of depositing layer was three. Considering the above-mentioned facts, a detailed investigation of the thickness optimization as well as the optimization of the dye loading time is an essential requirement to improve the performance of the cell. As per the previous investigations, thickness optimization and the effect of dye loading time have been observed in a separate investigation. In this investigation, we will show the effect of dye loading time on the DSSC performance at various photoelectrode thickness which has not been investigated earlier. The prime goal is to observe the optimized conditions of photovoltaic parameters in terms of dye loading time and photoelectrode thickness.

2. Experimental

2.1 Photoelectrode preparation

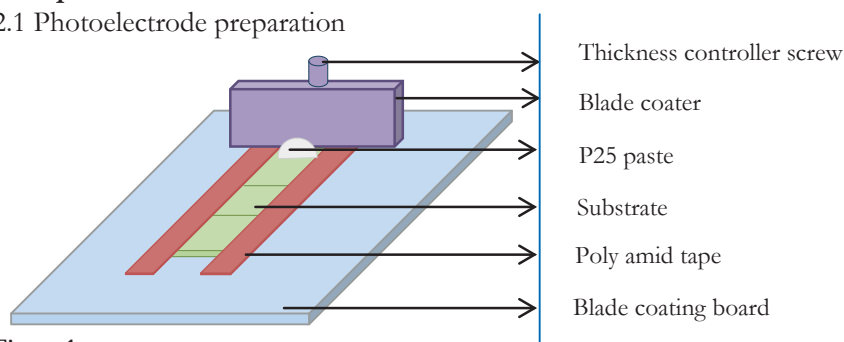


Figure 1
Blade coating arrangement

Photoelectrodes were prepared using the conventional Blade coating technique. The Blade coating paste was prepared using P25 type TiO_2 precursor in ethanol solvent. Blade coating past is prepared using 3 gm P25 nanoparticle in 6 ml ethanol solution. The solution was dispersed using an electronic homogenizer at 60% amplitude, and one-fourth pulse rate for 5 min. After the dispersion, the prepared paste was used for preparing the photoelectrode using the Blade coating technique. Along with the paste preparation, the fluorine-doped tin oxide (FTO) coated glass substrates were cleaned in an ultrasonic bath inside methanol solution two times and for acetone solution one time. An ultrasonic bath was used for 15 min for this cleaning purpose. Each of the conductive glasses ($2 \times 2 \text{ cm}^2$) was then dried by flowing nitrogen gas. After the nitrogen cleaning process, all the substrates were further cleaned by ozone (O_3) cleaning. After the cleaning process is over, the prepared paste is used to prepare the photoelectrode layer using the Blade coating technique. The blade coating arrangement is shown in Fig. 1. Three conductive FTO glass substrates were placed onto the Blade coating board which was fixed with the polyamide tape. Polyamide tape maintains the layer thickness to some extent. The thickness controller screw is adjusted properly to get the desired thickness. Before the coating, the paste is poured onto the FTO substrate's front side. Soon after that, the Blade coater is moved from front to back one time and from back to front another time to complete a single cycle. In this way, the first layer of metal oxide is prepared. After that, the coated layer is dried for a few minutes and the same process is repeated a second time. The prepared photoelectrodes are kept for dye loading.

2.2 Dye loading

For preparing the dye solution of 0.5 mM concentration, a 100 ml beaker is subsequently cleaned using methanol and ethanol in an ultrasonic bath. 0.0531 gm of ruthenium dye N719 is mixed with 90 ml ethanol solution and primarily mixed by gentle shaking. For complete dispersion, the solution is transferred to a glass bottle whose cover is sealed with paraffin tape and is kept in an ultrasonic bath at 45 Hz for 30 min inside the yellow room. In this way, the dye solution is ready for the experiment. Now, the prepared photoelectrodes emerged into the dye with the help of a substrate casing. For this investigation, the dye loading time was varied for 14, 18, 22, 30, 35, and 43 hours. During the dye loading, all the substrates inside the dye solution are kept in dark. After the estimated time is over, the photoelectrodes were taken out from the emerging dye and inserted into the methanol solution with gentle shaking to remove the extra dye or unwanted particles. In this way, the

photoelectrodes were prepared for cell fabrication.

2.3 Cell fabrication and characterization

The Pt-coated glass was used as the counter electrode of the cell. A 50 μm thick Polymer film was attached to the counter electrode having a space in the middle which provides space as well as encapsulates the electrolyte. The liquid electrolyte iodide/triiodide redox (Iodolyte AN-50, Solaronix) was carefully injected into that gap between the electrodes by a glass tube injector. Both of the electrodes were fixed with one another using two simple paper clips. The active area of the prepared photoelectrodes was about 4 cm^2 ($20 \times 20 \text{ mm}^2$) and its thickness was in the range of 10 to 20 μm as measured by a surface profilometer (Alpha step 500). Soon after the cell fabrication, the current-voltage (I - V) parameters were measured using a solar simulator (100 $\text{mW}\cdot\text{cm}^{-2}$, AM 1.5 illumination) in the air with a cell area of 0.16 cm^2 which was ensured by a still mask. The photoelectrode surface morphology was observed by a Scanning Electron Microscopy (SEM) image which was operated at 15 kV of operating voltage.

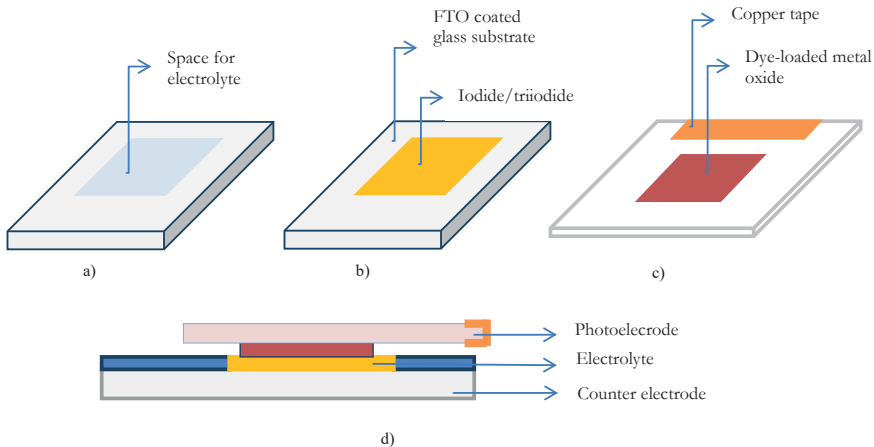


Figure 2

a) Pt-coated counter electrode, b) Pt-coated counter electrode with iodide/ triiodide solution, c) dye-loaded metal oxide FTO Photoelectrode, d) complete solar cell arrangement

3. Results and discussions:

Solar cell performance (I - V data) of various thicknesses (5 to 30 μm) with various dye loading times (10 to 26 h) has been investigated. Various performance parameters such as short circuit current density (J_{sc}) of the cells with various thicknesses and dye loading times to find the suitable thickness and dye loading time for P25-based DSSC. Additionally, the SEM image has

been analyzed to observe the surface morphology of the cells. Fig. 3 shows the current density of the cells at various thicknesses under different dye loading times. For

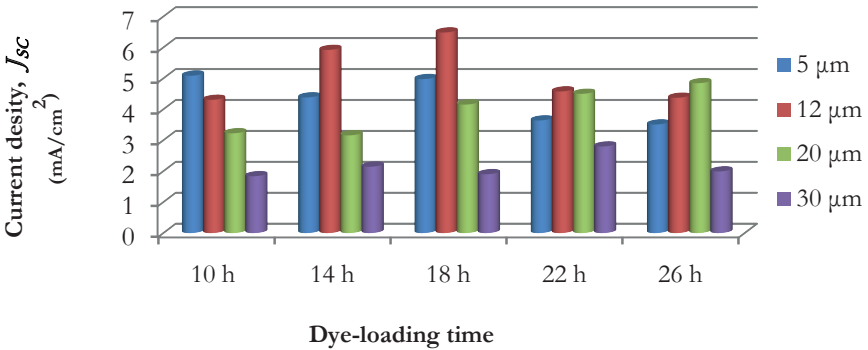


Figure 3
Current density for the cells of various thicknesses under different dye loading times

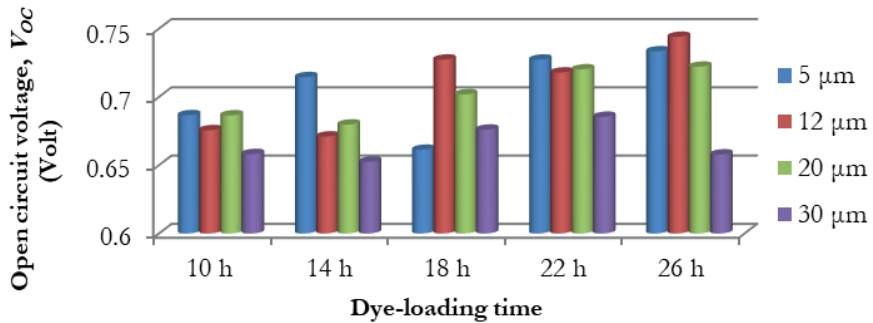


Figure 4
Open circuit voltage for the cells of various thicknesses under different dye loading times

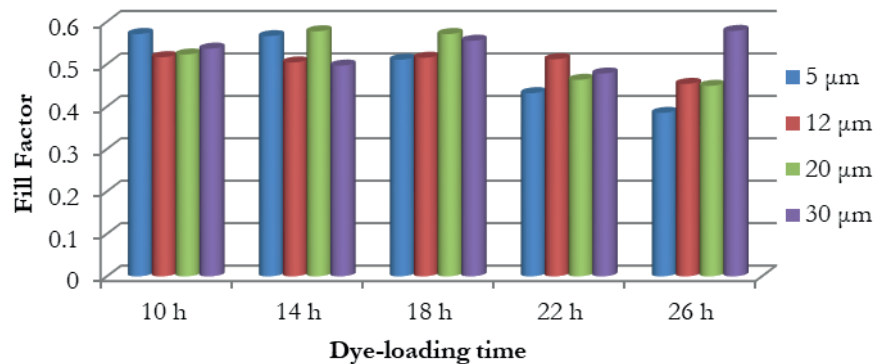


Figure 5
Fill Factor for the cells of various thicknesses under different dye loading times

lower dye loading times such as 10 h dye loading the maximum current density was found for a 5 μm thick layer cell. By maintaining 10 h dye loading, the current density was reduced for all the photoelectrode thickness cells. The maximum current density was found for 12 μm cells when the dye loading time was 14, 18, and 22 h. When the dye loading time was 26 h, the maximum current density was found for the 20 μm thick cell. Therefore, from this figure, it is evident that higher thickness requires more optimum dye loading time. However, by comparing both dye loading time and thickness the 12 μm thickness gives the best current

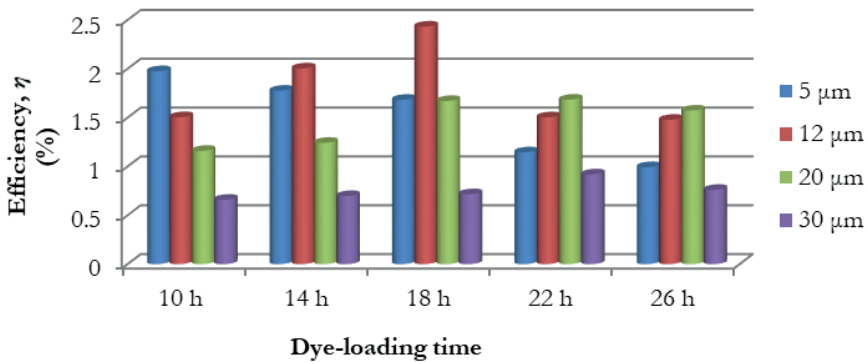


Figure 6

Overall power conversion efficiency for the cells of various thicknesses under different dye loading times

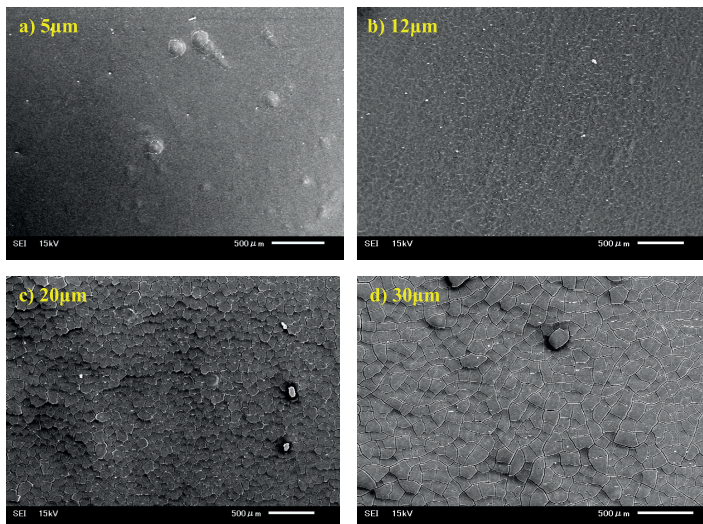


Figure 7

SEM image of P25 photoelectrode layer for various thicknesses of a) 5 μm , b) 12 μm , c) 20 μm , and d) 30 μm

density for 18 h dye loading condition. Again, the open circuit voltage (V_{oc}) for various cells under different thicknesses and dye loading times are presented in Fig. 4. V_{oc} is higher for the cells having lower photoelectrode thickness (except 12 μm thick cell) under various dye loading times. For a 12 μm cell, the highest open circuit voltage is found for 18 h dye loading time. Fig. 5 shows the fill factor data. For the dye loading time of 10, 14, and 18 h the fill factor was better for any thickness. Therefore, the dye loading time of more than 18 h is not suitable in terms of the fill factor of P25-based DSSC. Finally, the overall power conversion efficiency (η) data for the cells under the above-mentioned conditions of dye loading time and thickness are presented in Fig. 6. Combining all the effects of thickness and dye loading time on the performance parameters of the cells, the overall power conversion efficiency was better for lower thickness (5 and 12 μm) photoelectrode cells for the dye loading time of 10, 14, and 18 h. By summarizing all the results, the optimum condition is 12 μm and 18 h dye loading time for this investigation. Also, the surface morphologies for the photoelectrode surface of various thicknesses are shown in Fig. 7. From the image, it is evident that up to 12 μm thickness the photoelectrode layer does not have any crack on the surface. On the other hand, a huge amount of crack is found for 20 and 30 μm thick layers. The formation of cracks creates air spaces which in turns, reduces the average surface area for the dye-loading. Therefore, the average dye loading will reduce. Though, a higher thickness offers greater dye loading but the formation of crack will initiate more leakage current which will reduce the overall power conversion. Thus, the SEM image supports the $I-V$ data.

4. Conclusion

In this investigation, P25-based dye-sensitized solar cells of varying thicknesses have been fabricated using doctor blade method. For each photoelectrode thickness several samples were taken for various dye-loading times. $I-V$ and SEM data for the DSSCs of various thicknesses with varying dye loading time confirms that up to 12 μm thickness gives a crack-free stable photoelectrode layer. Greater thickness requires more dye loading time to get optimum photovoltaic performance. When the photoelectrode thickness is over 12 μm , there were several cracks on the photoelectrode surface which causes lower photovoltaic performance. Besides, a dye-loading time of more than 18 h causes aggregation of dye particles which in turn enhances the recombination rate and reduces the overall power conversion efficiency of the cells. In summary, the achieved photovoltaic parameters for the various dye loading times confirm that 12 μm thickness and 18 h dye loading time are suitable for P25-based DSSC.

References

- Abuelwafa, A. A., Choudhury, M. S. H., Dongol, M., El-Nahass, M. M., & Soga, T. (2018). The efficiency of ZnO/platinum octaethylporphyrin (PtOEP) nanocomposite photoanode at dye-sensitized solar cells. *Journal of Materials Science: Materials in Electronics*, 29 (16), 14232-14238.
- Babar, F., Mehmood, U., Asghar, H., Mehdi, M. H., Khan, A. U. H., Khalid, H., ... & Fatima, Z. (2020). Nanostructured photoanode materials and their deposition methods for efficient and economical third generation dye-sensitized solar cells: A comprehensive review. *Renewable and Sustainable Energy Reviews*, 129, 109919.
- Choudhury, M. S. H., Kato, S., Kishi, N., & Soga, T. (2017). Nickel tetraphenylporphyrin doping into ZnO nanoparticles for flexible dye-sensitized solar cell application. *Japanese Journal of Applied Physics*, 56(4S), 04CS05.
- Choudhury, M. S. H., Kishi, N., & Soga, T. (2015a). Effects of compression at elevated temperature for electrophorically deposited TiO₂-based dye-sensitized solar cell. *Japanese Journal of Applied Physics*, 55(1S), 01AE13.
- Choudhury, M. S. H., Kishi, N., & Soga, T. (2015b). Performance analysis of electrophorically deposited ZnO-based dye-sensitized solar cells prepared using compression at elevated temperature along with post-annealing. *Japanese Journal of Applied Physics*, 55(1S), 01AA16.
- Choudhury, M. S. H., Kishi, N., & Soga, T. (2016a). Compression of ZnO nanoparticle films at elevated temperature for flexible dye-sensitized solar cells. *Journal of Alloy and Compounds*, 656, 476-480.
- Choudhury, M. S. H., Kishi, N., & Soga, T. (2016b, June 5-10). *Hot-compression: An Effective Postdeposition Treatment for Electrophoretically Deposited Dye-sensitized Solar Cell*. Paper presented at the 2016 IEEE 43rd Photovoltaic Specialists Conference (PVSC), (pp. 1632-1637), Portland, Oregon, USA.
- Choudhury, M. S. H., Kishi, N., & Soga, T. (2016c). Hot-compress: A new postdeposition treatment for ZnO-based flexible dye-sensitized solar cells. *Material Research Bulletin*, 80, 135-138.
- De Marco, L., Manca, M., Giannuzzi, R., Malara, F., Melcarne, G., Ciccarella, G., ... & Gigli, G. (2010). Novel preparation method of TiO₂-nanorod-based photoelectrodes for dye-sensitized solar cells with improved light-harvesting efficiency. *The Journal of Physical Chemistry C*, 114(9), 4228-4236.
- Etxebarria, I., Ajuria, J., & Pacios, R. (2015). Polymer: fullerene solar cells: Materials, processing issues, and cell layouts to reach power conversion efficiency over 10%. *Journal of Photonics for Energy*, 5(1), 057214.

- Fan, J., Li, Z., Zhou, W., Miao, Y., Zhang, Y., Hu, J., & Shao, G. (2014). Dye-sensitized solar cells based on TiO₂ nanoparticles/nanobelts double-layered film with improved photovoltaic performance. *Applied Surface Science*, 319, 75–82.
- Hossain, M. K., Pervez, M. F., Mia, M. N. H., Mortuza, A. A., Rahaman, M. S., Karim, M. R., ... & Khan, M. A. (2017). Effect of dye extracting solvents and sensitization time on photovoltaic performance of natural dye sensitized solar cells. *Results in physics*, 7, 1516-1523.
- Iwata, S., Shibakawa, S., Imawaka, N., & Yoshino, K. (2018). Stability of the current characteristics of dye-sensitized solar cells in the second quadrant of the current–voltage characteristics. *Energy Reports*, 4, 8–12.
- Lee, C. P., Li, C. T., & Ho, K. C. (2017). Use of organic materials in dye-sensitized solar cells. *Materials Today*, 20(5), 267-283.
- Li, J., & Zhang, J. Z. (2009). Optical properties and applications of hybrid semiconductor nanomaterials. *Coordination Chemistry Reviews*, 253(23-24), 3015-3041.
- Lin, Y. P., Lin, S. Y., Lee, Y. C., & Chen-Yang, Y. W. (2013). High surface area electrospun prickle-like hierarchical anatase TiO₂ nanofibers for dye-sensitized solar cell photoanodes. *Journal of Materials Chemistry A*, 1(34), 9875-9884.
- Lindström, H., Holmberg, A., Magnusson, E., Lindquist, S. E., Malmqvist, L., & Hagfeldt, A. (2001). A new method for manufacturing nanostructured electrodes on plastic substrates. *Nano letters*, 1(2), 97-100.
- Luo, J., Gao, L., Sun, J., & Liu, Y. (2012). A bilayer structure of a titania nanoparticle/highly-ordered nanotube array for low-temperature dye-sensitized solar cells. *RSC Advances*, 2(5), 1884-1889.
- Magiswaran, K., Norizan, M. N., Mahmed, N., Mohamad, I. S., Idris, S. N., Sabri, M. F. M., ... & Salleh, M. A. A. M. (2022). Controlling the Layer Thickness of Zinc Oxide Photoanode and the Dye-Soaking Time for an Optimal-Efficiency Dye-Sensitized Solar Cell. *Coatings*, 13(1), 20.
- Meen, T. H., Tsai, J. K., Tu, Y. S., Wu, T. C., Hsu, W. D., & Chang, S. J. (2014). Optimization of the dye-sensitized solar cell performance by mechanical compression. *Nanoscale Research Letter*. 9, 523.
- O'Regan, B., & Gratzel, M., (1991). A low-cost, high-efficiency solar cell based on dye-sensitized colloidal TiO₂ films. *Nature*, 353, 737–740.
- Qiu, L., Ono, L. K., & Qi, Y (2018). Advances and challenges to the commercialization of organic-inorganic halide perovskite solar cell technology.

Materials Today Energy, 7, 169–189.

- Rahman, M. M., Islam, N., Alam, M. S., Uddin, M. A., Soga, T., & Choudhury M. S. H. (2022, February 26-27). *Optimization of Electrophoretic Deposition Parameters for Uniform ZnO Deposition on Conductive Glass Substrate*. Paper presented at 3rd Int. Conf. on Innovations in Science, Engineering and Technology (ICISSET), Chittagong, Bangladesh.
- Rajab, F. M. (2016). Effect of solvent, dye-loading time, and dye choice on the performance of dye-sensitized solar cells. *Journal of Nanomaterials*, 2016, 3703167.
- Sun, K. C., Qadir, M. B., & Jeong, S. H. (2014). Hydrothermal synthesis of TiO₂ nanotubes and their application as an over-layer for dye-sensitized solar cells. *RSC Advance* 4, 23223.
- Tammy, P. C., Qifeng, Z., & Guozhong, C. (2007). Effects of dye loading conditions on the energy conversion efficiency of ZnO and TiO₂ dye-sensitized solar cells. *Journal of Physical Chemistry C*, 111, 18808-18811.
- Tan, B. & Wu, Y. (2006). Dye-Sensitized Solar Cells Based on Anatase TiO₂ Nanoparticle / Nanowire Composites. *Journal of Physical Chemistry B*, 110, 15932.
- Wu, D., Zhu, F., Li, J., Dong, H., Li, Q., Jiang, K., & Xu, D., (2012). Monodisperse TiO₂ hierarchical hollow spheres assembled by nanospindles for dye-sensitized solar cells. *Journal of Material Chemistry*, 22, 11665.